Citation: Oncogenesis (2012) **1**, e11; doi:10.1038/oncsis.2012.11

www.nature.com/oncsis

ORIGINAL ARTICLE

Constitutive activation of breast tumor kinase accelerates cell migration and tumor growth *in vivo*

S Miah, A Martin and KE Lukong

Breast tumor kinase (BRK) is a non-receptor tyrosine kinase overexpressed in most human breast tumors, including lymph node metastases, but undetected in normal mammary tissue or in fibroadenomas. The activity of BRK-like Src family tyrosine kinase, is regulated negatively by phosphorylation of C-terminal tyrosine 447. Although the kinase that regulates BRK activation has not been identified, we and others have previously shown that BRK-Y447F is a constitutively active variant. Because BRK-Y447F significantly enhances the catalytic activity of the enzyme, we investigated the role of the constitutively active BRK variant in tumor formation and metastasis. Using stable breast cancer cell MDA-MB-231 we observed significantly enhanced rates of cell proliferation, migration and tumor formation in BRK-Y447F stable cells compared with wild-type stable cell lines. Our results indicate full activation of BRK is an essential component in the tumorigenic role of BRK.

Oncogenesis (2012) **1,** e11; doi:10.1038/oncsis.2012.11; published online 7 May 2012

Subject Categories: molecular oncology

Keywords: breast tumor kinase; BRK; PTK6; breast cancer; tumor formation; xenograft

INTRODUCTION

Breast tumor kinase (BRK) is a non-receptor tyrosine kinase originally identified in a screen for tyrosine kinases expressed in human melanocytes and eventually cloned from a human breast carcinoma.[1–3] BRK is overexpressed in about 60–85% of human breast carcinomas, but not in normal mammary gland or benign lesions.[1,2,3–5] BRK overexpression has also been observed in other cancers.[6–11]

The encoded 451 amino-acid polypeptide of BRK is composed of Src homology domains 3 and 2 (SH3 and SH2), a kinase domain and a putative C-terminal regulatory tyrosine and displays a similar architecture to and has 30–40% sequence identity with Src kinases.[12] Unlike Src family kinases, BRK lacks the myristoylated N-terminal consensus sequence required for membrane anchorage and therefore localizes to the nucleus and the cytoplasm.[12] Like Src kinases, BRK is regulated by intramolecular interactions. It is locked in an inactive conformation by interaction of phosphorylated C-terminal tyrosine 447 with the SH2 domain and regulated positively by phosphorylation of tyrosine 342 in the catalytic domain.[13,14] C-terminal Src kinase is a characterized negative regulator of Src family kinases.[15]

Although a negative or positive regulator of BRK activity has not been identified, studies have indicated that BRK is activated upon stimulation of the epidermal growth factor receptor (EGFR) and insulin-like growth factor-I receptor (IGF-IR)[16,17] and we and others have shown that mutation of tyrosine 447 to phenylalanine results in a constitutively active variant of BRK whose activity is significantly higher than that of wild-type (WT) BRK.[13,14,16] This implies that the activation of BRK would significantly alter the functional dynamics of the enzyme.

To understand the cellular and physiological significance of full activation of BRK, we have first of all assessed the activity of various BRK mutants and generated stable cell lines expressing constitutively active BRK-Y44F. The stable cell lines were subjected to cell proliferation and migration assays. As the function of active BRK in tumors is not fully understood, we have also investigated the role of constitutively active BRK in tumor formation in xenograft mice.

We present evidence that full activation of BRK significantly enhances the cellular and physiological properties of BRK, which include cell proliferation, migration and tumor formation.

RESULTS

Tyr447Phe BRK mutant is significantly more active than the WT BRK

Previous studies from the Miller group have demonstrated that various BRK mutant forms displayed activities higher than WT BRK when expressed in human embryonic kidney 293 (HEK293) cells.[18] These included W44A, SH2 and SH3 deletion mutants (ΔSH2 and ΔSH3), Y342A, K219M and Y447F mutant (Figure 1a). Trp44 is a conserved residue in the SH3 domain previously shown to make contacts with proline residues in the linker region and further stabilize the inactive conformation of BRK. Mutation of Trp44 to alanine (W44A) has shown to abolish the SH3–Linker interaction[19] and enhance enzyme activity.[18] Autophosphorylated Tyr342 is necessary for full activation of BRK, while mutation of Lys219, an essential active site residue, to methionine abrogates catalytic activity.[18] To begin to understand the role of activated BRK in various cellular processes, we first generated green fluorescence protein (GFP)-tagged BRK WT and Y447F constructs. To ensure that the GFP tag does not interfere with the enzyme activity, we compared the activities of various non-tagged BRK constructs to

Department of Biochemistry, College of Medicine, University of Saskatchewan, Saskatoon, Saskatchewan, Canada. Correspondence: Dr KE Lukong, Department of Biochemistry, College of Medicine, University of Saskatchewan, 107 Wiggins Road, Saskatoon, Saskatchewan, Canada, S7N 5E5.
E-mail: Kiven.lukong@usask.ca
Received 27 February 2012; accepted 28 March 2012

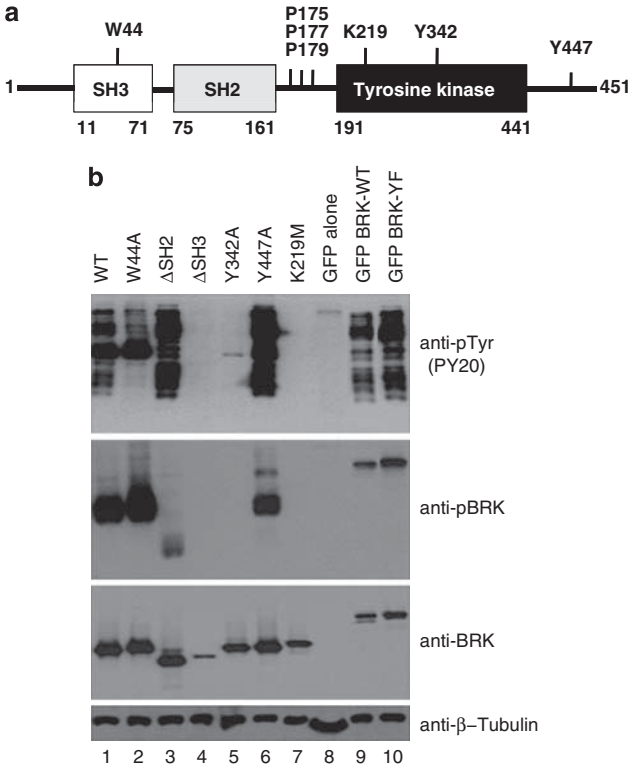

Figure 1. Tyr447Phe BRK mutant is significantly more active than the WT BRK. (**a**) Schematic representation of BRK. The diagram shows the functional domains and the positions of some of the keep residues mutated in this study.(**b**) Activity of BRK and BRK mutants in transfected HEK293 cells. WT BRK and BRK mutants, non-tagged and GFP-tagged, were transfected and expressed in HEK293 cells as described in 'Materials and methods'. The cells were transiently transfected with 0.1% PEI 'Max' (Polysciences Inc.) at a ratio of 3:1 reagent to DNA with the total amount of DNA being 2.5 μg per well in six-well dishes. Cells were washed 4 h after transfection, then cultured in DMEM containing 10% fetal calf serum for an additional 24 h. Cell lysates were subjected to SDS–PAGE and the proteins transferred onto nitrocellulose membranes and immunoblotted with antiphosphotyrosine antibody (PY20) and anti-BRK and anti-phospho-BRK (pTyr342). Anti-β-tubulin served as a loading control.

those of GFP-tagged constructs in transfected HEK293 cell lysates (Figure 1b). The lysates were subjected to SDS–PAGE analysis followed by immunoblotting using antiphosphotyrosine antibody, pY20, (Santa Cruz Biotechnology, Santa Cruz, CA, USA) designed specifically to recognized phosphorylated tyrsosine residues and using phospho-BRK designed to recognize autophosphorylation of BRK at Tyr342 (Millipore, Billerica, MA, USA). As previously shown by Qiu and Miller,[18] ΔSH3, K219M and Y342A mutants displayed significantly lower or no activity compared with WT as demonstrated by the degree of pY20 staining (Figure 1b, top panel, compare lanes 4, 5 and 7 to lane1). W44A showed a slightly lower activity than the WT. As anticipated, the ΔSH2 (lane 3) and Y447F (lane 6) variants displayed the highest levels of activity, confirming that docking of pY447 to the SH2 domain is equally important in BRK to stabilize an inactive conformation. In the context of the present work, it is important to note that both GFP-BRK-WT (lane 9) and GFP-BRK-Y447F (lane 10) display catalytic activity and that, as expected, GFP-BRK-Y447F showed a much higher level of substrate phosphorylation compared with GFP alone (lane 7) or GFP-BRK-WT (lane 9). These activity results using pY20 were corroborated with antiphospho-BRK staining, although it is not exactly clear why substrate phosphorylation by ΔSH2 was not detected by this antibody. Taken together, these data substantiate that BRK-Y447F is significantly more active than the WT and that a GFP tag does not interfere with catalytic activity.

Constitutively active BRK enhances mitogen-activated protein kinase (MAPK) activation and increases cell proliferation

To enable a better understanding of role of BRK in mammary cancers and to gain insight into the role that constitutively active BRK had on cell growth and cell proliferation, we generated three sets of stable cells, each set consisting of stably expressing GFP alone, GFP-BRK-WT and GFP-BRK-YF by retroviral infections. We utilized BRK-negative cell lines, which include epithelial cell lines MCF-10A and MDA-MB-231 (Figure 2a), as well as HEK293 cell line.[17] MCF-10A is an immortalized mammary epithelial cell line and MDA-MB-231 cells are estrogen receptor-negative, highly invasive breast cancer cell line. All of the cells were generated as pooled populations of puromycin-resistant cells to avoid any clonal variations. We subjected cell lysates from the stable cells to immunoblotting with anti-GFP and anti-BRK and demonstrate that stable MCF-10A express equivalent levels of GFP-BRK-WT and GFP-BRK-YF (Figure 2b). More importantly, we analyzed the cell lysates for their relative levels of tyrosine phosphorylation using antiphosphotyrosine antibody to ensure that the activity in the BRK-YF stable cells was significantly higher than the WT as expected. As shown in Figure 2c, overexpression of both BRK-WT and BRK-YF resulted in high phosphorylation of endogenous substrates compared with the control. As expected, BRK-YF stable cells display much higher levels of tyrosine kinase activity compared with BRK-YF samples (Figure 2c). Similar results were also obtained from both MDA-MB-231 and HEK293 stable cells (data not shown).

Kamalati *et al.*[20] demonstrated that exogenous expression of WT BRK in normal mammary epithelial cells enhanced mitogenic signaling. We and others have shown that epidermal growth factor (EGF)-induced activation of BRK contributed to the phosphorylation of BRK substrates Sam68 and paxillin.[17,21] Using our MCF-10A stable cell model system, we first investigated whether constitutive activation of BRK is accompanied by enhanced activation of mitogenic signaling in unstimulated cells. For this experiment, cell lysates from stable cell lines overexpressing GFP alone as control, GFP-BRK-WT and GFP-BRK-YF, as well as parental cell line were analyzed by immunoblotting for MAPK (extracellular-regulated kinase, Erk1/2) activation (Figure 2d). Indeed, MAPK activation as demonstrated by the level of MAPK phosphorylation was observed in both GFP-BRK-WT and GFP-BRK-YF samples (Figure 2d). As hypothesized, the presence of constitutive active BRK-YF resulted in a more pronounced activation of MAPK compared with the WT counterpart. The GFP-control cell lysates only showed background pMAPK cells compared with both the WT and YF. These data demonstrate that overexpression of BRK results in the activation of MAPK signaling even in the absence of EGF stimulation. Moreover, BRK activation was found to induce a significantly enhanced phosphorylation of MAPK and hence mitogenic signaling.

Since activation of the Ras/MAPK pathway has a pivotal role in cell proliferation and is associated with a gain-of-function mechanism in breast carcinogenesis,[22] we next examined the effect of constitutive activation of BRK on cell growth. The MCF-10A cell lines were plated at low density and cell number counted every 6 h for 48 h. Compared with the WT and control cell lines, we observed a significant increase in cell number in the pools of cells expressing BRK-YF as early as 6 h after the cells were plated (Figure 2e). A more modest MAPK activation and increased cell growth was also observed in MDA-MB-231 cells stably expressing BRK-YF (data not shown). No significant difference in cell viability was observed between the different cell types (data not shown). Taken together, these data show that BRK is an upstream effector in the MAPK pathway and constitutive activation of BRK results in increased MAPK activation that corresponds with enhanced cell growth.

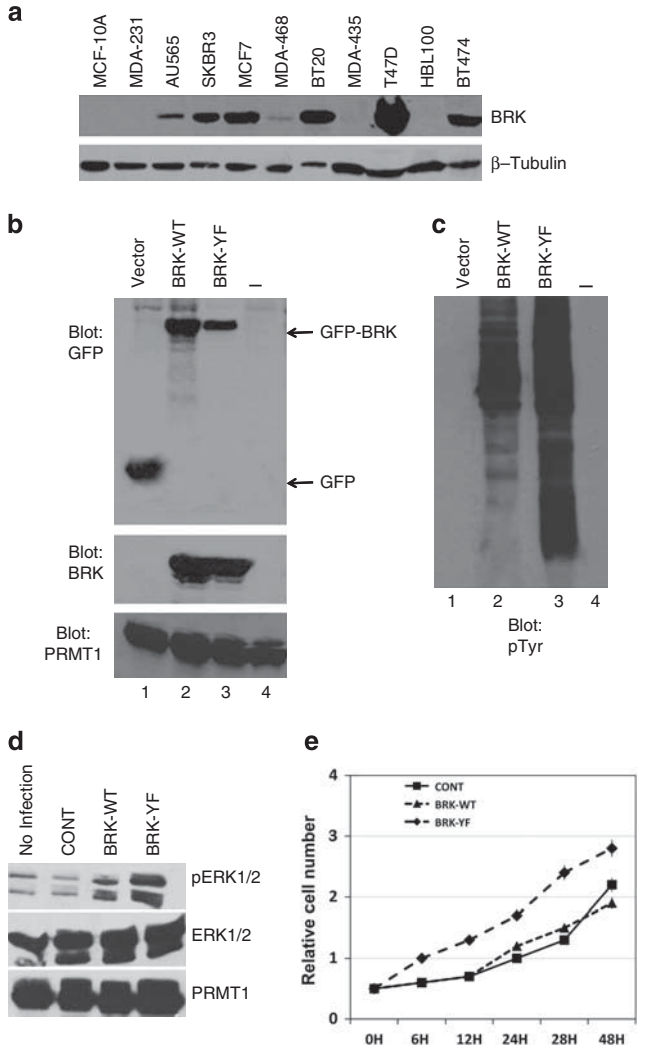

Figure 2. Constitutively active BRK enhances MAPK activation and increases cell proliferation. (**a**) BRK is not expressed in normal mammary gland epithelial cell lines. BRK expression in the indicated breast cancer cell lines (lanes 3–7) and normal mammary epithelial cell lines (lanes 1 and 2) was detected by immunoblotting. β-Actin was used as a loading control. (**b**, **c**) Immunobloting analysis of total cell lysates from MCF-10A stable cell lines showed increased activity of BRK-YF compared with WT and controls. MCF-10 A cells (5×10^5 cells) were infected with the retroviral viruses expressing GFP alone and GFP-BRK-WT and GFP-BRK-YF fusions. Stable populations were selected with 2 μg/ml puromycin and GFP expression detected by fluorescence microscopy and immunobloting with anti-GFP antibodies (lanes 1–3). Expression of ubiquitous protein arginine methyl transferase 1 (PRMT1) served as a loading control. (**c**) Stable cell lysates were analyzed by immunoblotting using antiphosphotyrosine antibody, 4G10. Significantly more activity was detected in BRK-YF cell lysates (lane 3) compared with the WT (lane 2) or the controls (lanes 1 and 4). The same results were obtained with MDA-231 and HEK293 stable cells (Supplementary Figure 1). (**d**, **e**) Activation of MAPK and increased cell growth in BRK-YF MCF-10A stable cells. (**d**) ERK1/2 activation (pERK1/2) was observed in both BRK-WT and YF stable cell lysates (lanes 3 and 4) and highest activity occurred in the BRK-YF stable cells. Expression of ubiquitous protein PRMT1 served as a loading control. (**e**) Growth assay shows higher growth rate in MCF-10A cells stably expressing BRK-YF than in the WT and vector-alone control stable cell lines.

Constitutive activation of BRK is associated with increased cell migration and invasion

Several studies have shown that BRK contributes to the processes of migration and invasion that characterize metastatic potential of breast cancers. For example, it has been previously shown that BRK can contribute to cell migration and proliferation by enhancing EGF-mediated phosphorylation of paxillin and activation of Rac1 via CrkII.[21] Similarly, BRK knockdown by RNA interference was shown to impair migration of breast cancer cells.[17,23,24] To address the role of constitutive activation of BRK on cell migration, we employed both the wound-healing and Boyden chamber migration assays. Cells were induced to migrate into a wound created by scratching confluent cultures with a pipette tip to examine the migration of MDA-MB-231 stable cell lines expressing GFP alone, GFP-BRK-WT or GFP-BRK-YF (Figure 3). MDA-MB-231 were selected for this experiment because of their characterized high migratory potential. Closure of wounded area was monitored for 36 h. As shown in Figure 3, the open area was rapidly covered by the BRK-WT and BRK-YF cells in comparison with vector control cells. Moreover, constitutively active BRK-YF accelerated wound closure more efficiently at 24 h than the BRK-WT cells (Figure 3a). The BRK-YF cells migrated into the wounded area and almost completely closed the wound within 48 h. Quantification of wound closure is represented in bar diagram in Figure 3b. The quantified open area in vector control cells were reduced from 100% to only 81%, BRK-WT cells were shrunk from 100 to 24%, whereas the constitutively active BRK-YF cells were dramatically reduced from 100 to 6% (Figure 3b). These data suggest that activation of BRK significantly accelerates motility of the MDA-MB-231 cells.

To validate the effects of BRK on cell migration by wound healing, we silenced BRK in two BRK-positive BT20 and SKBR3. BT20 expresses very low or no HER2 (human epidermal growth factor receptor 2), whereas SKBR3 highly overexpresses HER2.[25] To achieve stable BRK knockdown, the cells were transfected with lentiviral vector plasmids encoding BRK-specific short hairpin RNAs (shRNAs) and cell lysates analyzed by immunoblotting using anti-BRK antibodies (Figures 4a and d). The knockdown BRK was quantified to 33% in BT20 cells and to 13% in SKBR3 cells compared with scramble control or parental cell lines (Figures 4a and d, right panels). The confluent cell lines were scratched and wound healing was examined over a period of 48 h. As shown in Figures 4b and e, BRK knockdown resulted in a significant delay in wound closure compared with control cells after 48 h. The quantified score of open area showed that open area in the control cells was reduced from 100 to 17% after 48 h, whereas BRK knockdown BT20 cells only reduced to 56% (Figure 4c). Similarly, in SKBR3 control cells the area was reduced from 100 to 23% and only to 57% in the knockdown cells (Figure 4e). These data suggest that silencing of BRK abrogated motility of breast cells irrespective of their molecular subtype.

As an independent means of measuring cell motility, we further investigated the contribution of activated BRK in cell migration *in vitro* by employing the Transwell migration assays. These assays were performed using MDA-MB-231 cells stably expressing BRK-WT and BRK-YF and breast cancer cell lines BT20 and SKBR3 in which BRK is stably depleted. For each assay, the stable cells including the controls were each plated in the upper chamber in serum-free media. An 8 μm polycarbonate membrane separated the upper chamber from a lower chamber containing complete media. After 24 h incubation cells on the top of the membrane were removed by swiping and the membrane was rinsed and stained with hematoxylin. Migrated cells on the underside of the membrane were counted under a microscope, in four different viewing fields, at 20 × magnification. As shown Figure 5a, both BRK-WT and BRK-YF induced a dramatic increase in cell migration compared with the GFP alone as control or the parent cell line. BRK-WT enhanced migration by about two-folds more than the controls, while BRK-YF induced a marked increase in cell migration by over three-folds compared with the control cells. To further validate the involvement of BRK in migration, we performed Transwell migration assays with BT20 and SKBR3 stably depleted

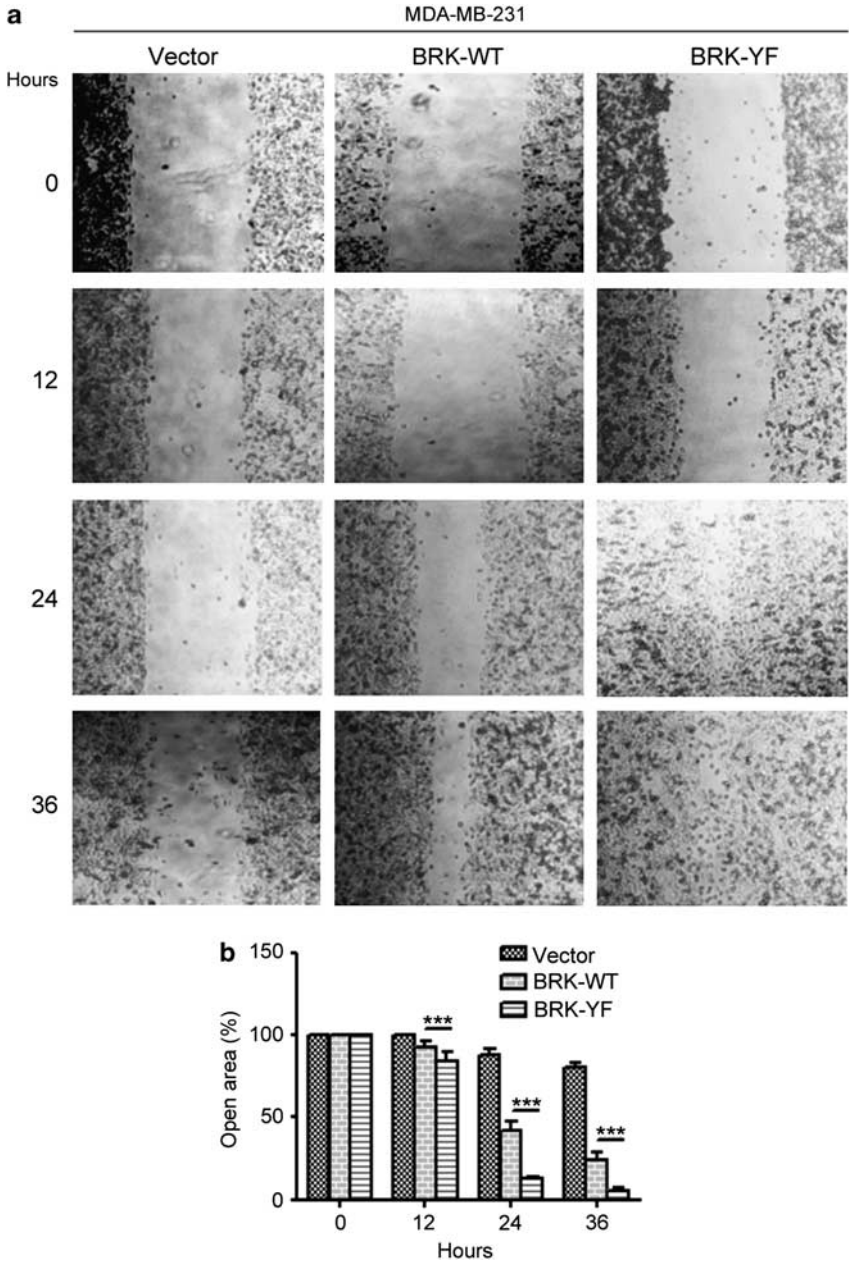

Figure 3. Constitutive activation of BRK accelerates cell migration in wound-healing assays. (**a**) MDA-MB-231 stable cell lines generated by infection with retroviruses expressing GFP-tagged BRK WT, or constitutively active BRK-YF or GFP as described in 'Materials and methods' and cell migration analyzed by using the wound-healing assay. Cells seeded into 6-well plates at 80–90% confluency. The wound of approximately 1 mm in width was scratched with a 200 μl pipette tip. Wound closure was monitored at the indicated time intervals and imaged with phase contrast microscopy on an inverted microscope (Olympus 1 × 51 using a 10 × phase contrast objective). The migration assay was performed in three independent experiments. (**b**) The open area (scratch) was quantified with TScratch software.[49] The *P*-values were determined for control and stably transfected cells and set at $^{***}P \leqslant 0.0001$ for statistically significance.

off BRK by shRNA (Figures 5b and c). As expected, in both BT20 and SKBR3 cell lines migration was attenuated by $>50\%$ in BRK-shRNA-expressing cells compared with the control shRNA cell lines or the parental cell lines. Collectively, these data suggest that BRK contributes to the basal migration of BT20 and SKBR3 cells and also that full activation of BRK is a strong proponent of BRK-induced cell migration.

Activated BRK promotes tumorigenicity *in vitro* and *in vivo*

Growth in anchorage-independent conditions is a hallmark of tumorigenicity and invasiveness in several cancer cell types.[26,27] As we have shown that constitutively active BRK enhances proliferation and migration of stable MDA-MB-231 cells, we considered whether BRK activation might provide an anchorage-independent growth advantage in soft agar in our MDA-MB-231stable cell model (Figure 6). Notably, we observed that the ability of BRK-YF stable MDA-MB-231 cells to form colonies was five times greater than the parental MD-MB-231 (Figure 6b), indicating the importance of BRK activation in malignant transformation and hence tumorigenesis.

We corroborated these findings in *in vivo* studies using an athymic mouse model system. The mammary fat pad of these mice ($n=4$ mice per group) were hence injected with MDA-MB-

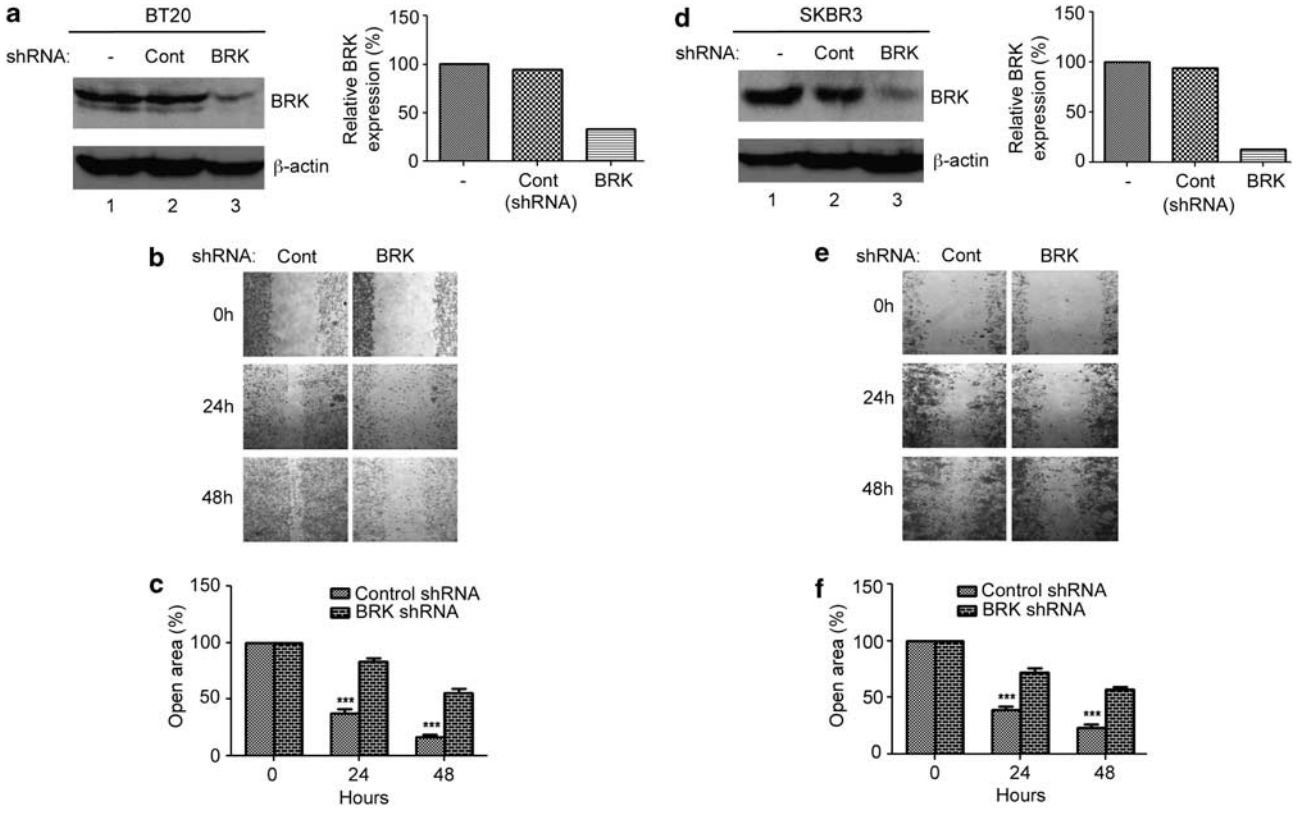

Figure 4. Stable knockdown of BRK significantly suppresses migration of breast cancer cells in wound-healing assays. Stable BRK knockdown were performed on parental breast cancer cell lines, BT20 and SKBR3 using shRNA lentiviral vector plasmids from Santa Cruz biotechnology according to the manufacture's protocol. (**a**, **d**) Efficient knockdown of BRK in breast cancer cells. BT20 and SKBR3 cells were transfected with a GFP-expressing plasmid or control shRNA plasmid or an shRNA-BRK plasmid using the PEI transfection method (See 'Materials and methods'). The GFP-control plasmid (lane 1, right and left panels) allowed the confirmation of the transduction efficiency by expressing GFP, detectable by fluorescence microscopy. The control shRNA plasmid (lanes 2) encode a scrambled shRNA sequence, which does not lead to mRNA degradation. BRK-shRNA lentiviral vector plasmid (lanes 3) comprises at least three lentiviral vector plasmids target-specific 19–25 nucleotides in shRNAs designed to knockdown *BRK* gene expression. Transfected cells were selected using puromycin. (**b**, **e**) BRK knockdown significantly suppresses migration of both BT20 and SKBR cells. The stable knockdown cells were analyzed for cell migration using the wound-healing assay in 6-well plates as described in Figure 3 legend. (**c**, **f**) The open area (scratch) was quantified with TScratch software.[49] The *P*-values were set at $***P \leqslant 0.0001$ for statistically significance.

231 cells stably expressing GFP alone, GFP-BRK-WT or GFP-BRK-YF. The mice were monitored for tumor formation and tumor volume measured every 7 days for 60 days (Figures 7a and b). All mice started developing palpable tumors 10 days after injection, and there was no significant difference in the latency period. However, in mice injected with GFP-BRK-YF-expressing cells, we observed a significantly faster growth rate compared with animals injected with the control cells (GFP alone) or the WT BRK (GFP-BRK-WT). At 60 days after injection, the average volume of tumors induced by GFP-BRK-YF-expressing cells was 2450 mm^3 compared with 1130 mm^3 for BRK-WT and 958 mm^3 for the control (GFP alone) group (Figure 7b). Primary tumors were excised at necropsy and weighed and tumor weights were compared across the groups (Figure 7c). In line with the final tumor volume data, we observed a significantly higher average weight of the BRK-YF-expressing tumors (3.25 g) compared with BRK-WT (1.04 g) and the control (0.81 g) (Figure 7d). These results demonstrate that the activation of BRK significantly enhances tumourogenicity and suggest that the enzymatic activity of BRK is essential in BRK-regulated breast cancer tumor progression.

DISCUSSION

Breast cancer is the most common female malignancy in the world with approximately one million new cases reported each year and it represents about 7% of all cancer-related deaths worldwide.[28] The critical importance of BRK in breast tumorigenesis is suggested by the fact that BRK is expressed in most breast carcinomas, but not normal mammary epithelium, making it a viable therapeutic target. BRK is overexpressed in 60–85% of breast tumors or cancer cell lines,[29] which is significant compared with approximately 20% of overexpression of HER2 protein in breast tumors. HER2 overexpression has been repeatedly identified as a poor prognostic factor.[30]

BRK is a tyrosine kinase with a functional architecture and modes of regulation reminiscent of Src family kinases. Similar to Src kinases, BRK is regulated negatively by phosphorylation of C-terminal tyrosine 447 (which is analogous to the regulatory Y530 of human Src) and positively by phosphorylation of tyrosine 342 in the catalytic domain (as Y419 of human Src).[13,14] C-terminal Src kinase phosphorylates the C-terminal tyrosine of Src kinases, promoting intramolecular interactions that lock the Src kinases in an inactive conformation.[15] Therefore, Tyr530-Phe mutation or dephosphorylation activates Src.[31] This dephosphorylation is often accompanied by autophosphorylation of pTyr419 within the activation loop, and results in a 10-fold increase in kinase activity.[32] Prevention of autophosphorylation by Tyr419-Phe mutation suppresses this activation by about fve-folds,[33,34] demonstrating the importance of synergy in Src activation. Therefore, the classical activation pathway of Src includes

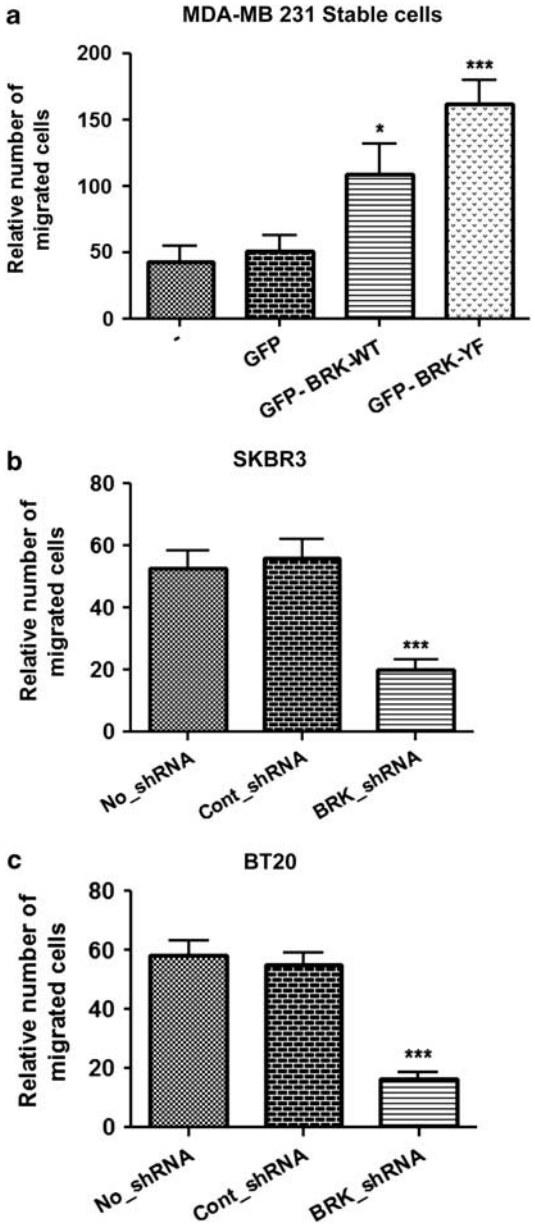

Figure 5. Transwell assays demonstrating the effect of BRK on cell migration. (**a**) Migration of BRK stable MDA-MB-231 cell lines expressing GFP-BRK-WT, or constitutively active GF-BRK-YF or GFP alone were evaluated in 24-well transwell polystyrene membrane with 8 μm size pores (See ' Materials and methods'). Migrated cells were fixed with paraformaldehyde, stained with crystal violet for 30 min and the number of migrating cells was counted scored in relative units. (**b**, **c**) BRK knockdown significantly suppresses migration of BT20 and SKBR breast cancer cell lines. The stable knockdown cells were prepared as described in Figure 4 legend and analyzed for migration by transwell assay as described above. All results are the mean (± s.e.m.) of more than three separate experiments. Statistical analysis $*P<0.05$, $***P<0.0001$.

dephosphorylation of Y530 to initiate a configuration change of the protein (partial activation) that promotes full activation by autophosphorylation of tyrosine site 419. The transmembrane receptor protein tyrosine phosphatase has been shown to activate Src by five-fold by dephosphorylating both pTyr530 and pTyr419 *in vivo*.[35] Clinically, dephosphorylated Y530Src is associtated with early stages of carcinogenesis in breast cancer patients.[36]

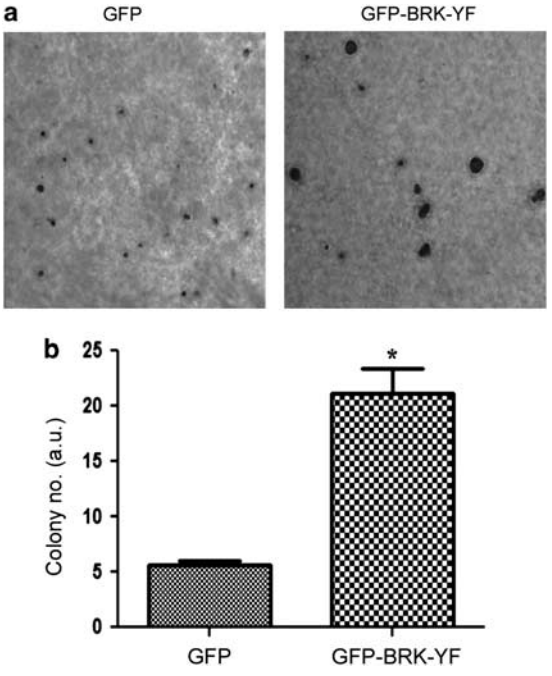

Figure 6. BRK activation promotes anchorage-independent growth of breast cancer cells. (**a**) Representative images of colony formation assay of MDA-MB-231 cells stably expressing control GFP or GFP-BRK-YF. 1×10^5 cells were suspended in soft agar and photographed after a 3-week incubation at 37 °C. (**b**) Cell colonies were counted in triplicate wells from five fields and mean of colonies were graphically represented. s.d. are indicated. Statistical analysis $*P<0.05$.

As the negative and positive regulators of BRK activity have not been identified, we generated constitutively an active mutant of BRK by mutating Tyr447 to Phe in this study to investigate the role of full activation of BRK on the oncogenic properties of BRK. We first evaluated the activities of various GFP-tagged and non-tagged BRK mutants and determined that in both cases certain mutant forms of BRK, including BRK-YF displayed higher activity than WT BRK when transfected into HEK293 cells (Figure 1b) and as previously demonstrated.[18,37] We next generated three sets of stable cell lines overexpressing GFP-BRK-WT and fully activated GFP-BRK-Y447F, as well as a GFP alone control (Figure 2b). The cell lines selected for these studies included HEK293 cells, immortalized mammary epithelial cell line MCF-10A and highly invasive breast cancer cell line, MDA-MB-231. These cell lines express little or no BRK (Figure 2a). We observed hyperactivation in BRK-YF stable cell lines compared with BRK-WT and controls (Figure 2c). Using our stable cell lines, we present evidence that support a critical role for BRK activity in the promotion oncogenic processes such as cell proliferation and migration, and tumor formation *in vivo*.

Mitogenic signaling involves the sequential activation of a MAPK kinase kinase (MAPKKK), a MAPK kinase (MAPKK) and the MAPK.[22] All four MAPK signaling cascades have been implicated in breast cancer. They are the ERK 1/2 pathway, the ERK5 pathway, the p38 pathway and the c-Jun N-terminal kinase pathway.[22,38] ERK 1/2 is significantly activated in a large subset of mammary tumors[39] and persistent activation of ErbB2 oncogene in MCF-10A is associated with activation of ERK 1/2[40]. Previous studies have demonstrated that exogenous expression of BRK enhanced EGF-induced proliferation of normal mammary epithelial cells EGF.[41] We previously demonstrated that phosphorylation of BRK substrate Sam68 upon EGF stimulation is partly BRK-dependent.[17] Here, we show that full activation of BRK results significantly higher cell growth associated with hyperactivation of ERK 1/2 (Figures 2d and e), consistent with a recent report published

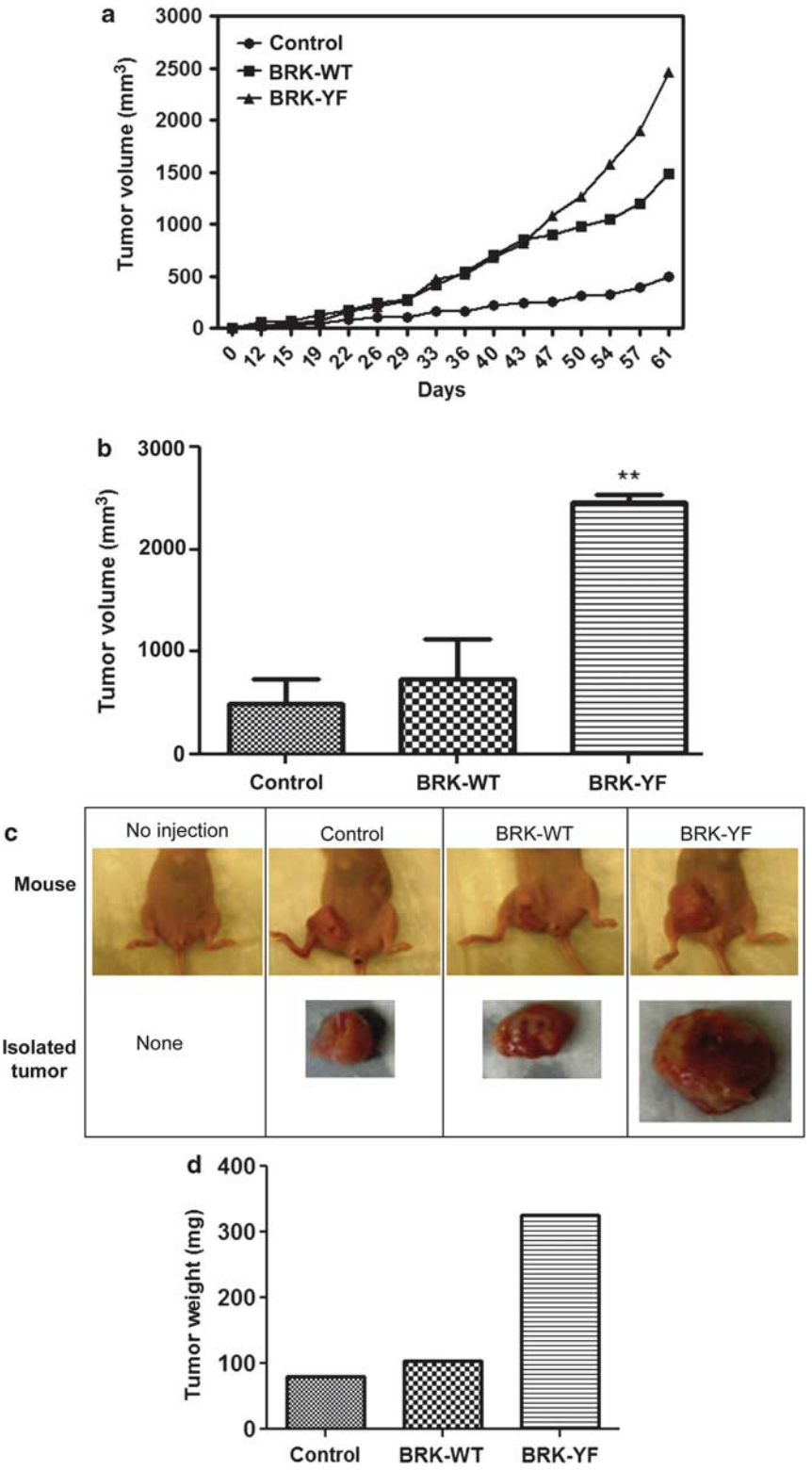

Figure 7. Overexpression of constitutively active BRK significantly enhanced xenograft tumor growth as compared with WT or control vector. (**a**) 2.5×10^6 MDA-MB-231 cells were injected subcutaneously bilaterally into mammary fat pads of four animals injected per cell line. Palpable tumors were monitored and measured bi-weekly for about 8 weeks. Tumor volume was calculated as follows $0.50 \times \text{length} \times \text{width}^2$. (**b**) The average volume of tumors induced by GFP-BRK-YF-expressing cells was 2450 mm^3 compared with 1130 mm^3 for BRK-WT and 958 mm^3 for the control (GFP alone) group. (**c**) A representative image of mice at endpoint showing the presence or absence of tumors at site of injection in mammary tissue. (**d**) The tumors of these mice at endpoint were isolated and weighed and the average weights were represented graphically. Statistical analysis. $^{**}P \leqslant 0.001$.

during the preparation of this manuscript.[42] We did not observed any effect of BRK on the activation of ERK5, p38 or c-Jun N-terminal kinase (data not shown) although Ostrander *et al.*[24] have previously shown that BRK regulates ERK5 and p38 activation albeit in heregulin-induced conditions.

Accumulating evidence has highlighted the importance of BRK in cell migration. For instance, BRK activation downstream of the EGFR resulted in increased Rac1 activity, associated with migration and invasion programs in both skin and breast cancer cell lines.[21] A recent study indicated that BRK silencing in HER2-positive breast cancer cell lines BT20 and JIMT1 results in decreased HER2 activation and reduced cell migration. Here, we used both the wound-healing and transwell assays to show that stable knockdown of BRK in both HER2-positive and negative cell lines BT20 and SKBR3, respectively, results in reduced cell migration (Figures 4, 5b and c). This implies that BRK can regulate cell migration in an EGFR-independent pathway. Similarly, stable expression of WT BRK and constitutively active BRK in HER2-negative MDA-MB-231 significantly increased cell migration (Figures 3 and 5a). We also confirmed the transforming potential of the Y447F mutant by evaluating the capacity of our stable cell lines for anchorage-independent growth. Consistent with previous reports, stable expression of BRK-YF resulted in a significant size of colonies formed in soft agar.[41,43]

The dramatic effect of constitutively active BRK on cell growth, cell migration and malignant transformation led us to examine whether activation of BRK was essential for the tumor formation *in vivo*. We transplanted our engineered MDA-MB-231 stable cell lines into immunocompromised mice, and measured tumor volume over time (Figure 7). We show that full activation of BRK promotes a more rapid tumor growth compared with the WT counterpart or the control. Overexpression of WT BRK was previously shown by Shen *et al.*[44] to promote tumor growth in animal, but our data stresses the importance of BRK activity in the promotion of tumor growth.

The exact mechanism by which BRK promotes migration and tumorigenesis is not known. We have shown that BRK may regulate these processes via activation of the Raf1-MEK1/2 –ERK1/2 cascade as demonstrated by hyperphosphorylation of ERK1/2 in BRK stable cell lines (Figure 2e). Other studies have suggested that BRK promotes cell migration and invasion through p190RhoGAP phosphorylation that results in Ras activation.[44] Therefore, because BRK regulates various signaling cascades, it is possible that BRK may mediate tumor-promoting events via a direct or an indirect contribution to transcription control. We have therefore performed microarray studies using our various stable cell lines to begin to understand the effect of BRK or BRK activation on differential gene expression (Supplementary Figure S1 and Tables S1 and S2). Dramatic effect was obtained with HEK293 cells where we observed gene expression differences between the control and the BRK-WT or BRK-YF as high as 160-folds. Upregulated genes included *CCD1*, *BOP1*, *CD44*, *CHCHD2* and *RLP19*, and the downregulated genes included *CTNNB1* and *MMP10* (Supplementary Figure S1). The validation of these targets and targets from MDA-MD-231 and MCF-10A stable cell lines are in progress.

Overall, the present study demonstrates that overexpression of constitutively active BRK highly correlates with exaggerated cell proliferation and ultimately, with increased transformation potential of epithelial cells. We have demonstrated for the first that full activation of BRK is an essential component in the promotion of tumorigenesis by BRK *in vivo*. Therefore, it can be predicted that BRK hyperactivation human breast cancers might exhibit an aggressive clinical behavior. We know from a recent study that mammary-targeted expression of WT BRK promoted infrequent mammary tumors with delayed latency.[45] On the basis of our results, the question of whether activated BRK is capable of directly inducing mammary gland tumors is feasible. Furthermore, many studies have reported that elevation of Src activity in human tumors including breast cancer correlates with disease stage and poor prognosis.[46,47] Hence, future profiling of the BRK activation in a large cohort of breast tumor samples may enable the use of BRK activation as a diagnostic or prognostic marker, and inhibition of BRK activity or activation as a viable therapeutic strategy in breast cancer treatment.

MATERIALS AND METHODS

Cell cultures

MDA-MB-231, HEK293, BT20 and SKBR3 cells were originally obtained from the American Type Culture Collection (ATCC, Manassas, VA, USA). The cells were cultured in high glucose (4.5 g/l), Dulbecco's modified Eagle's medium (DMEM) supplemented with 10% bovine calf serum (Thermo scientific, Logan, USA) and containing 4 mM L-glutamine, 100 units/ml penicillin, 100 μg/ml streptomycin (Sigma-Aldrich, St Louis, MO, USA). MCF-10A cells (ATCC) was cultured in DME/F-12 1:1(1 ×) medium (Thermo scientific) containing 5% horse serum (Sigma-Aldrich), 20 ng/ml EGF(Upstate, Lake Placid, NY, USA), 0.5 μg/ml hydrocortisone (Sigma-Aldrich), 100 ng/ml cholera toxin (Sigma-Aldrich), 50 U/ml penicillin, and 50 mg/ml streptomycin as well as 10 ng/ml insulin (Sigma-Aldrich), as described by Debnath *et al.*[48]

Antibodies

The following antibodies were purchased from Santa Cruz Biotechnology: anti-BRK (N19, sc-916), anti-ERK1/2 (sc-1647), anti-pERK1/2 (sc-16982), anti-GFP (sc-8334), anti-pTyr PY20 (sc-508), anti-p-p38 (sc-17852-R), anti-p38 (sc-535) and anti-b-actin (sc-130300). Both antiphosphotyrosine (anti-pTyr) clone 4G10 and anti-pBRK (Y342) were from Upstate. Anti-PRMT1 antibody was obtained from Millipore (Billerica, MA, USA).

Mammalian cell expression

HEK293 cells were maintained in DMEM containing 10% fetal bovine serum, 50 U/ml of penicillin–streptomycin. Cells were rinsed and supplemented with a fresh serum-free culture medium just before transfection. The cells were transiently transfected with 0.1% Polyethylenimine 'Max' (PEI) (Polysciences Inc., Warrington, PA, USA) at a ratio of 3:1 reagent to DNA with the total amount of DNA being 2.5 μg per well in six-well dishes. For each well, 2.5 μg of DNA was added to 107.5 μl of sterile 0.15M NaCl in a microcentrifuge tube and vortexed gently for 10 s. 15 μl 0.1% PEI was added to the DNA mixture and vortexed gently for 10 s. The DNA–PEI complex was then incubated for 10 min at room temperature. The mixture was added dropwise to wells containing 2 ml of complete media and the plates were incubated at 37 °C. Cells were washed 4 h after transfection, then cultured in complete media for an additional 16–48 h.

Generation of stable cell lines

Transduction and generation of stable cell pools amphotropic HEK293-derived Phoenix packaging cells were used to package pBabe-puro retroviral system. For retrovirus production, packaging cells were cultured on 10-cm gelatin-coated plates in 10 ml of DMEM medium supplemented with 10% bovine calf serum. Transfection with 1% PEI (Polysciences Inc) was conducted with 10 μg of retroviral DNA in 60 μl of 1% plus 430 μl of 0.15M NaCl for the 100 mm culture plates. Virus-containing supernatant was collected at 24 h and 48 h timepoints, filtered through 0.45 μm syringe filter, aliquoted and stored at − 80 °C. To infect MDA-MB-231 cells, virus-containing supernatant was supplemented with polybrene (Source), and overlaid on the target cells. After overnight incubation with the viral supernatant, this was changed to fresh culture medium. Pools of MDA-MB-231 cells stably expressing GFP alone, GFP-BRK-WT and GFP-BRK-YF fusions were selected with puromycin (Sigma-Aldrich). Expression of EGFP from the GFP-tagged BRK was detected by fluorescence microscopy 48–72 h after infection. To produce stable BRK knockdown cell line we used BRK-expressing parental cell lines BT20 and SKBR3. This knockdown experiment was performed according to the manufactures protocol by using shRNA lentiviral vector plasmids from Santa Cruz Biotechnology. The shRNA plasmids generally consist of a pool of three to five lentiviral vector plasmids each encoding target-specific 19–25 nt shRNAs designed to knockdown gene expression. As controls, non-infected BT20 and SKBR3 cells (mock) and BT20 and SKBR3 cells were infected with a control shRNA and a GFP-control plasmid were used. shRNA were transfeted into those

cells to deplete endogenous Brk. A set of three shRNAs were used to complete this knockdown process. (1) GFP-control plasmid that allowed the confirmation of the transduction efficiency by expressing GFP, detectable by fluorescence microscopy. (2) Control shRNA plasmid that encode a scrambled shRNA sequence, which does not lead to the specific degradation of any mRNA. (3) BRK-shRNA lentiviral vector plasmid, which contains target-specific 19–25 nucleotides in shRNAs designed to knock-down *BRK* gene expression. Transfected cells were selected using puromycin (Sigma-Aldrich).

Cell migration (wound-healing) assay

Cells were seeded into six-well plates at a density of 1×10^6 cells/well and cultured until confluent 80–90% in culture medium. A 1000 μl sterile pipette tip was used to longitudinally straight scratch a constant-diameter stripe in the confluent monolayer. The medium and cell debris were aspirated away and replaced with a fresh culture medium. After wounding 0, 12, 24, 36 and 48 h later plates were imaged using Olympus 1×51 inverted microscope (Olympus America, Center Valley, PA, USA) with a $10\times$ phase contrast objective. These experiments were repeated with duplication. Values were means ± s.d. from at least two independent experiments.

Transwell assay

The cells were cultured in serum-free medium overnight, harvested and resuspended into serum-free medium. A suspension of cells (5×10^5cells) was added to upper chamber of 24-well Transwell plates (Corning Incorporated, Corning, NY, USA) and a complete medium (containing 10% fetal bovine serum) was added into the bottom chamber of Transwell (6.5 mm diameter and 8.0 μm thick). Then the cells were incubated at 37 °C and 5% CO_2 for 24 h, the non-migrated cells were removed by using a sterile cotton swab from the upper surface of the filter. The migrated cells through the chamber onto the lower surface of the filter were fixed with paraformaldehyde and stained with crystal violet for 30 min. The number of migrating cells was counted (Five high power fields were counted per filter to score for migration) under Olympus 1×51 microscope and the count was scored as migration in comparison with parental control cells.

Soft agar anchorage-independent growth assay

MDA-MB-231 cells were suspended in a top layer of DMEM-10% calf serum containing 0.35% low melting point agarose (Sigma-Aldrich) at 42 °C and overlaid onto the solidified 0.6% agarose layer containing DMEM–10% fetal bovine serum. After 3 weeks of incubation at 37 °C, the numbers of colonies formed were counted in triplicate wells from five fields photographed with a $10\times$ objective.

Mouse tumorigenicity assay

Xenograft experiments were conducted in 6–7-week-old female athymic nude mice, purchased from the National Cancer Institute, Frederick, MD, USA. MDA-MB-231 cells expressing each of the GFP-BRK fusions including GFP alone as stable pools were harvested in PBS and resuspended in Matrigel (BD Biosciences, Bedford, MA, USA). For each injection, 2.5×10^6 MDA-MB-231 cells in a 100 μl volume of Matrigel were injected subcutaneously bilaterally into mammary fat pads number 5 according to standard injection procedures, with four animals injected per cell line. Once tumors were palpable (about 2 weeks after injection of tumor cells), mammary primary tumor growth rates were monitored and analyzed by measuring tumor length (L) and width (W), for about 8 weeks. Tumor size was assessed by measurements with an electronic caliper. Volume was calculated as $0.50 \times \text{length} \times \text{width}^2$. Nude mouse xenograft experiments were performed under animal protocol approved by the Animal Care Unit and Committee of the University of Saskatchewan. Mice were killed in a humane manner when the tumor size exceeded the approved limit by animal ethical authority.

Immunoblotting

Total cell lysate prepared from transfected or non-transfected cells was subjected to SDS 10% polyacrylamide gel electrophoresis (SDS–PAGE), and electrophoresed proteins were transferred to nitrocellulose membranes (Bio-RAD, Hercules, CA, USA). In general, membranes were blocked for 30–45 min in 5% non-fat dry milk or in 1.0% of bovine serum albumin when phosphotyrosine antibodies are used. The membranes were incubated overnight at 4 °C with primary antibodies prepared according to manufacturer's instructions. Polyclonal goat HRP-conjugated secondary antibodies against mouse or rabbit (Bio-Rad Inc., 1:10 000 dilution) were incubated on membranes for 1 h at 4 °C, followed by chemiluminescence detection using the ECL kit (DuPont, Wilmington, DE, USA) and protein bands were visualized by autoradiography.

Statistical analysis

For statistical analysis, one-way and two-way analysis of variance followed by a post hoc Newman–Keuls test was used for multiple comparisons using GraphPad Prism version 5.04 for Windows, GraphPad Software, San Diego, California, USA, www.graphpad.com. The results are given as the means ± s.d., $n \geqslant 3$ unless otherwise stated. $P \leq 0.05$ was considered statistically significant.

CONFLICT OF INTEREST

The authors declare no conflict of interest.

ACKNOWLEDGEMENTS

We thank Dr Miller for the generous gifts BRK constructs. This work was supported by funding from the Canadian Institutes of Health Research (CIHR). KEL is an investigator of the CIHR.

REFERENCES

1 Barker KT, Jackson LE, Crompton MR. BRK tyrosine kinase expression in a high proportion of human breast carcinomas. *Oncogene* 1997; **15**: 799–805.
2 Mitchell PJ, Barker KT, Martindale JE, Kamalati T, Lowe PN, Page MJ *et al.* Cloning and characterization of cDNAs encoding a novel non-receptor tyrosine kinase, brk, expressed in human breast tumours. *Oncogene* 1994; **9**: 2383–2390.
3 Aubele M, Auer G, Walch AK, Munro A, Atkinson MJ, Braselmann H *et al.* PTK (protein tyrosine kinase)-6 and HER2 and 4, but not HER1 and 3 predict long-term survival in breast carcinomas. *Br J Cancer* 2007; **96**: 801–807.
4 Mitchell PJ, Barker KT, Shipley J, Crompton MR. Characterisation and chromosome mapping of the human non receptor tyrosine kinase gene, brk. *Oncogene* 1997; **15**: 1497–1502.
5 Harvey AJ, Pennington CJ, Porter S, Burmi RS, Edwards DR, Court W *et al.* Brk protects breast cancer cells from autophagic cell death induced by loss of anchorage. *Am J Pathol* 2009; **175**: 1226–1234.
6 Easty DJ, Mitchell PJ, Patel K, Flørenes VA, Spritz RA, Bennett DC. Loss of expression of receptor tyrosine kinase family genes *PTK7* and *SEK* in metastatic melanoma. *Int J Cancer* 1997; **71**: 1061–1065.
7 Llor X, Serfas MS, Bie W, Vasioukhin V, Polonskaia M, Derry J *et al.* BRK/Sik expression in the gastrointestinal tract and in colon tumors. *Clin Cancer Res* 1999; **5**: 1767–1777.
8 Petro BJ, Tan RC, Tyner AL, Lingen MW, Watanabe K. Differential expression of the non-receptor tyrosine kinase BRK in oral squamous cell carcinoma and normal oral epithelium. *Oral Oncol* 2004; **40**: 1040–1047.
9 Derry JJ, Prins GS, Ray V, Tyner AL. Altered localization and activity of the intracellular tyrosine kinase BRK/Sik in prostate tumor cells. *Oncogene* 2003; **22**: 4212–4220.
10 Kasprzycka M, Majewski M, Wang ZJ, Ptasznik A, Wysocka M, Zhang Q *et al.* Expression and oncogenic role of Brk (PTK6/Sik) protein tyrosine kinase in lymphocytes. *Am J Pathol* 2006; **168**: 1631–1641.
11 Schmandt RE, Bennett M, Clifford S, Thornton A, Jiang F, Broaddus RR *et al.* The BRK tyrosine kinase is expressed in high-grade serous carcinoma of the ovary. *Cancer Biol Ther* 2006; **5**: 1136–1141.
12 Serfas MS, Tyner AL. Brk, Srm, Frk, and Src42A form a distinct family of intracellular Src-like tyrosine kinases. *Oncol Res* 2003; **13**: 409–419.
13 Derry JJ, Richard S, Carvajal HV, Ye X, Vasioukhin V, Cochrane AW *et al.* Sik (BRK) phosphorylates Sam68 in the nucleus and negatively regulates its RNA binding activity. *Mol Cell Biol* 2000; **20**: 6114–6126.
14 Qiu H, Miller WT. Regulation of the nonreceptor tyrosine kinase Brk by autophosphorylation and by autoinhibition. *J Biol Chem* 2002; **277**: 34634–34641.
15 Okada M, Nakagawa H. A protein tyrosine kinase involved in regulation of pp60c-src function. *J Biol Chem* 1989; **264**: 20886–20893.
16 Lukong KE, Richard S. Sam68, the KH domain-containing superSTAR. *Biochim Biophys Acta* 2003; **1653**: 73–86.
17 Lukong KE, Larocque D, Tyner AL, Richard S. Tyrosine phosphorylation of sam68 by breast tumor kinase regulates intranuclear localization and cell cycle progression. *J Biol Chem* 2005; **280**: 38639–38647.

18 Qiu H, Miller WT. Role of the Brk SH3 domain in substrate recognition. *Oncogene* 2004; **23**: 2216–2223.
19 Kim H, Jung J, Lee ES, Kim YC, Lee W, Lee ST. Molecular dissection of the interaction between the SH3 domain and the SH2-kinase linker region in PTK6. *Biochem Biophys Res Commun* 2007; **362**: 829–834.
20 Kamalati T, Jolin HE, Mitchell PJ, Barker KT, Jackson LE, Dean CJ *et al.* Brk, a breast tumor-derived non-receptor protein-tyrosine kinase, sensitizes mammary epithelial cells to epidermal growth factor. *J Biol Chem* 1996; **271**: 30956–30963.
21 Chen HY, Shen CH, Tsai YT, Lin FC, Huang YP, Chen RH. Brk activates rac1 and promotes cell migration and invasion by phosphorylating paxillin. *Mol Cell Biol* 2004; **24**: 10558–10572.
22 Krishna M, Narang H. The complexity of mitogen-activated protein kinases (MAPKs) made simple. *Cell Mol Life Sci* 2008; **65**: 3525–3544.
23 Harvey AJ, Crompton MR. Use of RNA interference to validate Brk as a novel therapeutic target in breast cancer: Brk promotes breast carcinoma cell proliferation. *Oncogene* 2003; **22**: 5006–5010.
24 Ostrander JH, Daniel AR, Lofgren K, Kleer CG, Lange CA. Breast tumor kinase (protein tyrosine kinase 6) regulates heregulin-induced activation of ERK5 and p38 MAP kinases in breast cancer cells. *Cancer Res* 2007; **67**: 4199–4209.
25 Neve RM, Chin K, Fridlyand J, Yeh J, Baehner FL, Fevr T *et al.* A collection of breast cancer cell lines for the study of functionally distinct cancer subtypes. *Cancer Cell* 2006; **10**: 515–527.
26 Tsatsanis C, Spandidos DA. Oncogenic kinase signaling in human neoplasms. *Ann NY Acad Sci* 2004; **1028**: 168–175.
27 Simpson CD, Anyiwe K, Schimmer AD. Anoikis resistance and tumor metastasis. *Cancer Lett* 2008; **272**: 177–185.
28 Bray F, McCarron P, Parkin DM. The changing global patterns of female breast cancer incidence and mortality. *Breast Cancer Res* 2004; **6**: 229–239.
29 Brauer PM, Tyner AL. Building a better understanding of the intracellular tyrosine kinase PTK6 - BRK by BRK. *Biochim Biophys Acta* 2010; **1806**: 66–73.
30 Rauser S, Marquardt C, Balluff B, Deininger SO, Albers C, Belau E *et al.* Classification of HER2 receptor status in breast cancer tissues by MALDI imaging mass spectrometry. *J Proteome Res* 2010; **9**: 1854–1863.
31 Hunter T. A tail of two src's: mutatis mutandis. *Cell* 1987; **49**: 1–4.
32 Boggon TJ, Eck MJ. Structure and regulation of Src family kinases. *Oncogene* 2004; **23**: 7918–7927.
33 Kmiecik TE, Shalloway D. Activation and suppression of pp60c-src transforming ability by mutation of its primary sites of tyrosine phosphorylation. *Cell* 1987; **49**: 65–73.
34 Piwnica-Worms H, Saunders KB, Roberts TM, Smith AE, Cheng SH. Tyrosine phosphorylation regulates the biochemical and biological properties of pp60c-src. *Cell* 1987; **49**: 75–82.
35 Pallen CJ. Protein tyrosine phosphatase alpha (PTPalpha): a Src family kinase activator and mediator of multiple biological effects. *Curr Top Med Chem* 2003; **3**: 821–835.
36 Elsberger B, Tan BA, Mallon EA, Brunton VG, Edwards J. Is there an association with phosphorylation and dephosphorylation of Src kinase at tyrosine 530 and breast cancer patient disease-specific survival. *Br J Cancer* 2010; **103**: 1831–1834.
37 Lukong KE, Huot ME, Richard S. BRK phosphorylates PSF promoting its cytoplasmic localization and cell cycle arrest. *Cell Signal* 2009; **21**: 1415–1422.
38 Wang X, Tournier C. Regulation of cellular functions by the ERK5 signalling pathway. *Cell Signal* 2006; **18**: 753–760.
39 Mueller H, Flury N, Eppenberger-Castori S, Kueng W, David F, Eppenberger U. Potential prognostic value of mitogen-activated protein kinase activity for disease-free survival of primary breast cancer patients. *Int J Cancer* 2000; **89**: 384–388.
40 Seton-Rogers SE, Lu Y, Hines LM, Koundinya M, LaBaer J, Muthuswamy SK *et al.* Cooperation of the ErbB2 receptor and transforming growth factor beta in induction of migration and invasion in mammary epithelial cells. *Proc Natl Acad Sci USA* 2004; **101**: 1257–1262.
41 Kamalati T, Jolin HE, Mitchell PJ, Barker KT, Jackson LE, Dean CJ *et al.* Brk, a breast tumor-derived non-receptor protein-tyrosine kinase, sensitizes mammary epithelial cells to epidermal growth factor. *J Biol Chem* 1996; **271**: 30956–30963.
42 Li X, Lu Y, Liang K, Hsu J-M, Albarracin C, Mills GB *et al.* Brk/PTK6 sustains activated EGFR signaling through inhibiting EGFR degradation and transactivating EGFR. *Oncogene* (e-pub ahead of print 9 January 2012; doi:10.1038/onc.2011.608).
43 Kim H, Lee ST. An intramolecular interaction between SH2-kinase linker and kinase domain is essential for the catalytic activity of protein-tyrosine kinase-6. *J Biol Chem* 2005; **280**: 28973–28980.
44 Shen CH, Chen HY, Lin MS, Li FY, Chang CC, Kuo ML *et al.* Breast tumor kinase phosphorylates p190RhoGAP to regulate rho and ras and promote breast carcinoma growth, migration, and invasion. *Cancer Res* 2008; **68**: 7779–7787.
45 Lofgren KA, Ostrander JH, Housa D, Hubbard GK, Locatelli A, Bliss RL *et al.* Mammary gland specific expression of Brk/PTK6 promotes delayed involution and tumor formation associated with activation of p38 MAPK. *Breast Cancer Res* 2011; **13**: R89.
46 Summy JM, Gallick GE. Src family kinases in tumor progression and metastasis. *Cancer Metastasis Rev* 2003; **22**: 337–358.
47 Elsberger B, Stewart B, Tatarov O, Edwards J. Is Src a viable target for treating solid tumours? *Curr Cancer Drug Targets* 2010; **10**: 683–694.
48 Debnath J, Muthuswamy SK, Brugge JS. Morphogenesis and oncogenesis of MCF-10A mammary epithelial acini grown in three-dimensional basement membrane cultures. *Methods* 2003; **30**: 256–268.
49 Geback T, Schulz MM, Koumoutsakos P, Detmar M. TScratch: a novel and simple software tool for automated analysis of monolayer wound healing assays. *Biotechniques* 2009; **46**: 265–274.

Supplementary Information accompanies the paper on the Oncogenesis website (http://www.nature.com/oncsis).